

RESEARCH

Open Access



Apparent diffusion coefficient values in Modic changes – interobserver reproducibility and relation to Modic type

Magnhild H. Dagestad^{1,2*}, Nils Vetti^{1,2}, Per M. Kristoffersen^{1,2}, John-Anker Zwart^{3,4}, Kjersti Storheim^{3,5}, Gunnstein Bakland⁶, Jens I. Brox^{4,7}, Lars Grøvlø⁸, Gunn H. Marchand^{9,10}, Erling Andersen¹¹, Jörg Assmus¹² and Ansgar Espeland^{1,2}

Abstract

Background: Modic Changes (MCs) in the vertebral bone marrow were related to back pain in some studies but have uncertain clinical relevance. Diffusion weighted MRI with apparent diffusion coefficient (ADC)-measurements can add information on bone marrow lesions. However, few have studied ADC measurements in MCs. Further studies require reproducible and valid measurements. We expect valid ADC values to be higher in MC type 1 (oedema type) vs type 3 (sclerotic type) vs type 2 (fatty type). Accordingly, the purpose of this study was to evaluate ADC values in MCs for interobserver reproducibility and relation to MC type.

Methods: We used ADC maps (b 50, 400, 800 s/mm²) from 1.5 T lumbar spine MRI of 90 chronic low back pain patients with MCs in the AIM (Antibiotics In Modic changes)-study. Two radiologists independently measured ADC in fixed-sized regions of interests. Variables were MC-ADC (ADC in MC), MC-ADC% (0% = vertebral body, 100% = cerebrospinal fluid) and MC-ADC-ratio (MC-ADC divided by vertebral body ADC). We calculated mean difference between observers ± limits of agreement (LoA) at separate endplates. The relation between ADC variables and MC type was assessed using linear mixed-effects models and by calculating the area under the receiver operating characteristic curve (AUC).

Results: The 90 patients (mean age 44 years; 54 women) had 224 MCs Th12-S1 comprising type 1 ($n = 111$), type 2 ($n = 91$) and type 3 MC groups ($n = 22$). All ADC variables had higher predicted mean for type 1 vs 3 vs 2 ($p < 0.001$ to 0.02): MC-ADC (10^{-6} mm²/s) 1201/796/576, MC-ADC% 36/21/14, and MC-ADC-ratio 5.9/4.2/3.1. MC-ADC and MC-ADC% had moderate to high ability to discriminate between the MC type groups (AUC 0.73–0.91). MC-ADC-ratio had low to moderate ability (AUC 0.67–0.85). At L4-S1, widest/narrowest LoA were for MC-ADC $20 \pm 407/12 \pm 254$, MC-ADC% $1.6 \pm 18.8/1.4 \pm 10.4$, and MC-ADC-ratio $0.3 \pm 4.3/0.2 \pm 3.9$. Difference between observers > 50% of their mean value was less frequent for MC-ADC (9% of MCs) vs MC-ADC% and MC-ADC-ratio (17–20%).

Conclusions: The MC-ADC variable (highest mean ADC in the MC) had best interobserver reproducibility, discriminated between MC type groups, and may be used in further research. ADC values differed between MC types as expected from previously reported MC histology.

*Correspondence: magnhild.hammersland.dagestad@helse-bergen.no

² Department of Clinical Medicine, University of Bergen, P.O. Box 7804, 5020 Bergen, Norway
Full list of author information is available at the end of the article



Keywords: MR-imaging, Spine, Imaging sequences, Adults, Skeletal-axial, Observer performance

Background

Diffusion-weighted magnetic resonance imaging (DWI) is based on the random motion or “self-diffusion” of water molecules in a tissue, which depends on its histology [1]. The apparent diffusion coefficient (ADC) is a measurement of the diffusion calculated from the DWI-images [1–3]. Thus, the ADC adds information on function (diffusion) not revealed by imaging of anatomy and histology. DWI was first successfully used to evaluate brain tissue and is now also used in other soft tissue organs, especially for cancer imaging. In the vertebral bone marrow, DWI and ADC measurements are not part of standard clinical imaging protocols but have been applied to study inflammatory and infectious disorders and to differentiate benign from malignant compression fractures [3–9].

Modic changes (MCs) are magnetic resonance imaging (MRI) findings of vertebral bone marrow changes extending from the endplate. They are divided into type 1 (oedema type), 2 (fatty type) and 3 (sclerotic type) based upon T1- and T2-weighted images [10]. Type 1 MCs were related to back pain in some studies [11–13], but the clinical significance of MCs is uncertain [14]. There are limited data on ADC measurements in MCs [4–6, 15], but ADC values have been used to help distinguish type 1 MCs from infectious spondylitis [4, 5] and inflammatory spondyloarthritis [6]. In patients with MCs, DWI represents a research tool and has yet no role in routine imaging. Further research on the relevance of ADC measurements in MCs requires reproducible and valid measurements. We expect valid ADC values to differ according to MC type, since the underlying histology differs [16]. The aim of this study was to evaluate ADC values in MCs for interobserver reproducibility and relation to MC type.

Methods

This cross-sectional study was based on baseline MRI of 90 consecutive patients aged 25–63 years (mean age 44 years; 54 women) with chronic low back pain and MCs who were included in the Norwegian AIM (Antibiotics In Modic changes)-study, which comprised 180 patients. The current sample size ($n=90$) was based on a power calculation (see below). Eligibility criteria and methodology of the AIM-study are previously published [17, 18]. In short, all AIM patients had type 1 and/or type 2 MCs, with height $\geq 10\%$ of vertebral body height and diameter > 5 mm, at the level of a previous lumbar disc herniation [17]. The present analysis included any type of MC of

that size at any level Th12-S1 with or without disc herniation. Patients with prior low back surgery, except surgery for disc herniation performed more than 1 year earlier, were excluded from the AIM-study. None had lumbar metal implants. All patients gave written informed consent prior to inclusion. The study was approved by the Regional Committees for Medical Research Ethics in South East Norway (ref. no. 2014/158). The current report follows guidelines for reporting reliability and agreement studies [19].

Images

The patients included in the present analysis underwent MRI of the lumbar spine during the initial phase of AIM from 2015 to 2016 at five centres using identical protocols and 1.5T scanners (Magnetom Avanto B19, Siemens Healthineers, Erlangen, Germany). This study applied sagittal ADC maps and T1- and T2-weighted non-fat saturated fast spin-echo images (“T1/T2”). Gradient-echo diffusion weighted echo-planar imaging with fat saturation was performed. The system software generated ADC maps based on b values of 50, 400 and 800 s/mm² (recommended by the vendor) and three orthogonal directions of diffusion sensitization (see protocol details in Table 1).

For T1/T2, slice thickness/ interslice gap was 4 mm/0.4 mm, matrix 384 × 269, field of view 300 mm × 300 mm, echo time (ms)/repetition time (ms) 11/575 (T1) and 87/3700 (T2), and echo train length 5 (T1) and 17 (T2). All images were stored and evaluated at a single centre using Agfa Impax 6.5 (Agfa Health-Care, Mortsel, Belgium).

Evaluation

Two radiologists (A, B), with 6 (A) and more than 10 years of experience (B), independently evaluated levels Th12-S1 (12 endplates) using all sagittal slices. The observers were aware that patients had chronic low back pain but were otherwise blinded to clinical findings. They cross-navigated between the ADC map and the T1/T2 images to ensure ADC was measured in an MC related area. MCs were defined based on T1/T2 images [10, 20] (Table 2). We excluded MCs with height $< 10\%$ of vertebral body height or diameter ≤ 5 mm according to one/both radiologists.

For each MC, ADC was measured in the MC related area that was most intense on the ADC map, in normal vertebral body marrow, and in cerebrospinal fluid (CSF) using a circular region of interest (ROI) with

Table 1 DWI with sagittal ADC maps of the lumbar spine

| | |
|--|------------------------------------|
| Repetition time (TR) | 5500 ms |
| Echo time (TE) | 104 ms |
| Echo-planar imaging (EPI) factor | 192 |
| Number of acquisitions (averages) | 3 |
| Number of concatenations | 1 |
| Number of slices | 17 |
| Matrix (frequency x phase) | 192 x 192 |
| Field of view (FoV) | 350 mm x 350 mm |
| Slice thickness | 4.0 mm |
| Interslice gap | 0.0 mm |
| Voxel size | 1.8 mm x 1.8 mm x 4.0 mm |
| Receiver bandwidth | 1628 Hz/pixel |
| Phase encoding direction | Anterior to posterior |
| Saturation pulses | Anterior, 30 mm |
| Acquisition time | 3 min 48 s |
| Coverage | From above Th12 to below S2 |
| Phase oversampling | 0% |
| Fat saturation technique | Chemical shift-selective pre-pulse |
| Parallel acquisition techniques (PAT) mode | None |
| Distortion correction filters | Yes |
| b values | 50, 400, 800 s/mm ² |
| Diffusion weightings (b values) | 3 |
| Diffusion encoding scheme | Bipolar |

DWI Diffusion weighted imaging, ADC Apparent diffusion coefficient

Sagittal gradient-echo diffusion weighted echo-planar imaging (EPI) with fat saturation was performed on 1.5T Magnetom Avanto scanners with B19 software (Siemens Healthineers, Erlangen, Germany). The system software generated ADC maps based on the three tabled b values and an average measure for the three orthogonal directions of diffusion sensitization. The integrated spine array coil was used, and no surface coils

predefined size (Fig. 1, Table 2). To limit variation in ADC measurements, we did not use freely shaped ROIs. If the MC area had uniform intensity on the ADC map, ADC was measured in the area where the MC had largest height on T1/T2.

The following ADC variables were analysed (Table 2): (a) the MC related ADC value (10^{-6} mm²/s) (MC-ADC), (b) MC-ADC in percent (MC-ADC%) where 0% = ADC in normal vertebral body marrow and 100% = ADC in CSF, and (c) MC-ADC divided by the vertebral body ADC (MC-ADC-ratio).

Prior to any ADC measurements, as part of a previous study [20], MC type was independently assessed by three radiologists (B, C, D), each with more than 10 years' spine MRI experience. MCs were classified in types 1, 2 and 3 [10] (Table 2).

Mixed MC types were classified as primary (most extensive) type / and secondary type, i.e., MC types 1/2, 1/3, 2/1, 3/1, 2/3 and 3/2. Finally, in the present study, MCs were grouped into a type 1 group (any MC containing type 1), type 2 group (pure type 2 MCs) or type 3 group (MC types 3, 3/2, and 2/3).

Conclusive MC type was based on the agreement of at least two of the three observers B, C, and D. If all three disagreed, MC type was decided in consensus with observer A. The conclusive value for ADC variables was the mean of the values reported by observers A and B. The height of the MC into the vertebral body was measured in mm in our previous study [20] and is reported here as the mean of the values reported by observers C and D.

Table 2 Description of magnetic resonance imaging variables

| | |
|--------------|--|
| MCs | Signal changes in the vertebral bone marrow that extend from the endplate. Excluded are changes separated from the endplate, abutting the endplate with a smaller base than height, or extending through the endplate (Schmorl's hernias). |
| MC type | MC type 1 is hypointense on T1- and hyperintense on T2-weighted images. Type 2 is hyperintense on T1 and hyper- or isointense on T2. Type 3 is hypointense on T1 and T2. Borderline type 1 vs 2 with near isointense T1 signal is rated as type 2. |
| MC-ADC | Highest mean ADC value in a 41.8 mm ² ROI in the vertebral body marrow at the endplate with MC on T1/T2. The ROI is placed in the most intense MC related region on the ADC map. If the MC region has uniform intensity on the ADC map, the ROI is placed in the MC area with largest height on T1/T2. ADC is not measured for MCs with height < 10% of vertebral body height or diameter ≤ 5 mm. A ROI of only 41.8 mm ² (diameter 7 mm) is used to accommodate small MCs. |
| CSF-ADC | Mean ADC value in the CSF in a 41.8 mm ² ROI at the level of the MC affected vertebral unit, measured in the midsagittal image, or the next image left or right, avoiding non-CSF structures (like nerve roots seen on T1/T2). CSF-ADC is measured in an area with uniform intensity and no pulsation artefacts, behind the lower half of the cranial vertebra of the vertebral unit (e.g., behind L3 if the MC is superior or inferior to the L3/L4 disc) if possible, and otherwise behind the caudal vertebra of the unit or at the next vertebral unit caudally or cranially. |
| Body-ADC | Mean ADC value in a 94 mm ² ROI in normal (on T1/T2) vertebral body marrow near the MC. The ROI is placed close to the endplate in the central anteroposterior third of the normal opposite part (caudally or cranially) of the vertebral body with the MC. If the opposite part is not normal, and always when the MC is in S1, the ROI is placed in the nearest vertebra above, in its caudal part if possible, and otherwise in its cranial part. The measurement is first considered in the midsagittal image and then, if necessary, considered in the next image (left or right) before a new location may be considered. The larger 94 mm ² ROI is used to average more pixels without including the central vertebral vein in the ROI. |
| MC-ADC-ratio | Calculated as MC-ADC / Body-ADC |
| MC-ADC% | Calculated as (MC-ADC – Body-ADC) x 100% / (CSF-ADC – Body-ADC) |

MC Modic change, ADC Apparent diffusion coefficient, ROI Region of interest, CSF Cerebrospinal fluid

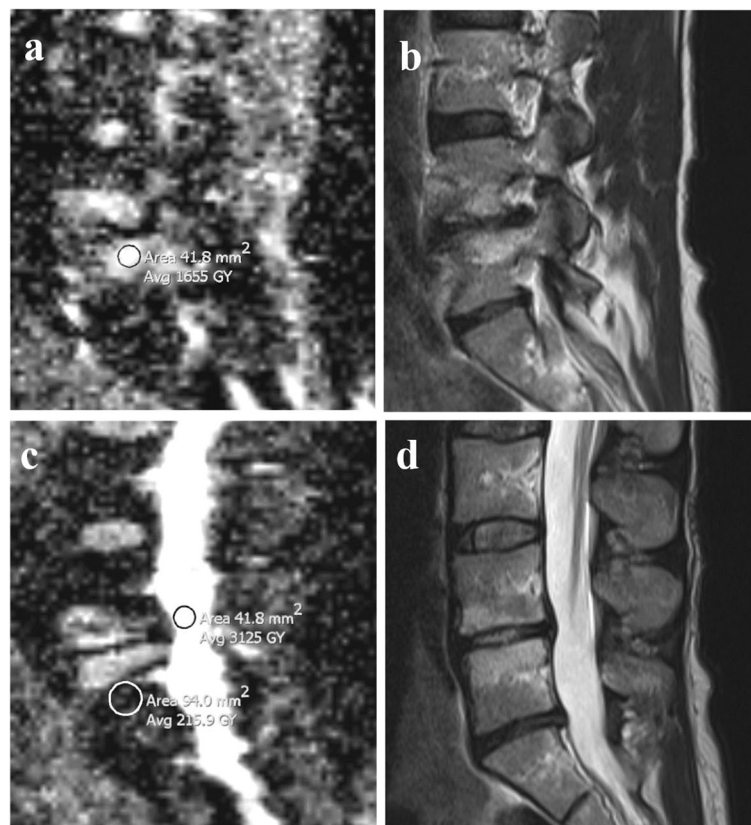


Fig. 1 Measurements of ADC values. (a–d) A 50-year-old woman with chronic low back pain. ADC maps (a, c) and corresponding T2 weighted fast spin echo images (b, d) showing MCs at the L4/L5 level. ADC measurements (Avg GY corresponding to mean 10^{-6} mm²/s) included (a) highest mean ADC value in the MC region (1655 in a 41.8 mm² ROI) and (c) mean ADC in normal vertebral body marrow (215.9 in a 94 mm² ROI) and in CSF (3125 in a 41.8 mm² ROI). Midsagittal images were used for measurements in CSF at the level of the MC and close to the endplate in normal vertebral body marrow near the MC. ADC, apparent diffusion coefficient. MC, Modic change. ROI, region of interest. CSF, cerebrospinal fluid

Pilot study

Prior to this study, observers A, B, and C performed a pilot study on 10 patients, to determine the ADC evaluation criteria and align the measurements. The pilot study patients were not included in the present study.

Hypothesis

A priori, we hypothesized that ADC values were higher in the type 1 MC group vs the type 3 group and higher in the type 3 group vs the pure type 2 group. Rationale: Compared to type 2 and 3, type 1 MCs are likely to contain more inflammatory oedema, favouring motion of water molecules and increasing the ADC value. Trabecular thickening / sclerosis restricts water motion, and less trabecular thickening in type 1 vs type 3 MCs [21] also suggests higher ADC values in type 1. The large hydrophobic fatty cells in type 2 MCs may restrict water motion / reduce ADC values more than does the fibrovascular granulation tissue with inflammatory cells in type 1 MCs [10, 16] and the trabecular thickening in type

3 MCs [21]. In an MC containing type 1 but also type 2 and/or 3, we expected type 1 to contribute the highest ADC value.

Statistical analyses

The reproducibility analysis was restricted to MCs extending from one of the four lowest endplates (L4–S1), because of low prevalence (<10%) of MCs at the other endplates [22]. Interobserver reliability at each endplate was assessed by Cohen's kappa (MC presence and type) and intraclass correlation coefficients (ICCs) (ADC variables). We used 2-way random effects, absolute-agreement, average-measures ICCs. ADC variables were also analyzed using Bland Altman plots with mean of differences ± 1.96 SD (limits of agreement, LoA) at each endplate and pooled across all four endplates L4–S1. We further calculated the proportion of differences exceeding 50% of the observers' mean value for each ADC variable across L4–S1. We used 50% as cut-off because LoA were $5\% \pm 45\%$ for ADC in vertebral bone marrow in

a prior intra rater study [23]. Interpretation of Cohen's kappa: 0.00–0.20 poor; 0.21–0.40 fair; 0.41–0.60 moderate; 0.61–0.80 good; 0.81–1.00 very good reliability [22]. ICC values were regarded to indicate poor (<0.50), moderate (0.50–0.75), good (0.76–0.90) or excellent (>0.90) reliability [24].

The relation between each ADC variable and MC type group was analysed using conclusive ADC values from MCs extending from one of the 12 endplates Th12-S1. Linear mixed-effects models were conducted using the ADC variable as dependent variable, MC type group as fixed effect, and endplate and patient as random effects. In each MC type group, the model returned a predicted mean value of the ADC variable that had been adjusted for data dependency between MCs at different endplates within the same patient. We also assessed the ability of each ADC variable to discriminate between the MC type groups by calculating the area under the receiver operating characteristic curve (AUC). We graded the discriminatory ability as low (AUC 0.5 to <0.7), moderate (0.7 to <0.9), or high (0.9–1.0) [25].

Mixed-effect models were conducted in R 4.0 (R Foundation, Vienna, Austria), using normality plots of standardized residuals and fitted values to assess model assumptions. All other analyses were performed using MedCalc 17.6 (MedCalc Software, Ostend, Belgium). Plots were made using Matlab 9.5 (Mathworks, Massachusetts, United States) and MedCalc 17.6. The significance level was 0.05.

Sample size

Previously reported ADC values (recalculated to 10⁻⁶ mm²/s) were 624–1800 (SD 120–316) in type 1 MCs [4, 5] and 500 (SD 160) in type 2 MCs [4]. Assuming SD 300 for ADC in both of two MC groups, 36 MCs in each group are sufficient to detect a mean ADC difference of 200 between the groups (β=0.2, two-sided α=0.05).

We needed 31 MCs at a given endplate to get a precision of ±0.10 (95% confidence level) for an ICC of 0.85. We expected 90 patients to have enough MCs to compare the ADC variables between the three MC type groups and to estimate their reliability.

Results

We included MCs from all 90 patients, 224 MCs in total (Table 3). These were 111 type 1 group MCs (any type 1), 91 type 2 group MCs (pure type 2), and 22 type 3 group MCs (20 type 2/3, 2 type 3/2, 0 type 3). MC height was mean 10.7 mm (SD 3.6 mm) and was ≥7 mm in 85% of the MCs (191/224). For reproducibility analyses, 201 MCs at L4-S1 were included.

Interobserver reproducibility

The interobserver reliability was very good (kappa 0.85–0.96) for MC presence but varied from moderate to very good (kappa 0.41–0.81) for MC type group (Additional file 1, Table A1) and good to excellent (ICC 0.84–0.98) for the three ADC variables (Table 4).

For MC-ADC, values (10⁻⁶ mm²/s) from both observers ranged from 108 to 2029 (mean 913) across the 201 MCs L4-S1. Widest LoA were 20 ± 407 (at L4-L5 inferior to disc) and narrowest LoA were 12 ± 254 (at L5/S1 inferior to disc) (Fig. 2).

MC-ADC% ranged from 6 to 76 (mean 25.6) and had widest and narrowest LoA of 1.6 ± 18.8 and 1.4 ± 10.4 (Fig. 3).

MC-ADC-ratio ranged from 0.5 to 15.6 (mean 4.7) with widest and narrowest LoA 0.3 ± 4.3 and 0.2 ± 3.9 (Fig. 4).

Pooled LoA across L4-S1 were for MC-ADC (10⁻⁶ mm²/s) 7 ± 316, MC-ADC% 1.2 ± 13.8, and MC-ADC-ratio 0.4 ± 4.0. The upper border of these LoA reached 35, 59, and 94% of the mean value for MC-ADC (913), MC-ADC% (25.6) and MC-ADC-ratio (4.7), respectively, across all 201 MCs L4-S1.

Table 3 Distribution of Modic types across the lumbar spine

| Modic type | Th12/L1 | L1/L2 | L2/L3 | L3/L4 | L4/L5 | L5/S1 | Total |
|------------|---------|---------|--------|-------|---------|----------|-----------|
| Pure 1 | 0 | 0 | 0 | 1 | 3 | 11 | 15 (7) |
| 1/2 | 0 | 0 | 2 | 4 | 19 | 20 | 45 (20) |
| 1/3 | 0 | 0 | 0 | 0 | 7 | 7 | 14 (6) |
| 2/1 | 0 | 0 | 3 | 0 | 8 | 25 | 36 (16) |
| 3/1 | 0 | 0 | 1 | 0 | 0 | 0 | 1 (0.4) |
| Pure 2 | 2 | 2 | 4 | 3 | 35 | 45 | 91 (41) |
| 2/3 | 0 | 0 | 1 | 0 | 7 | 12 | 20 (9) |
| 3/2 | 0 | 0 | 0 | 0 | 0 | 2 | 2 (0.9) |
| Pure 3 | 0 | 0 | 0 | 0 | 0 | 0 | 0 |
| Total | 2 (0.9) | 2 (0.9) | 11 (5) | 8 (4) | 79 (35) | 122 (54) | 224 (100) |

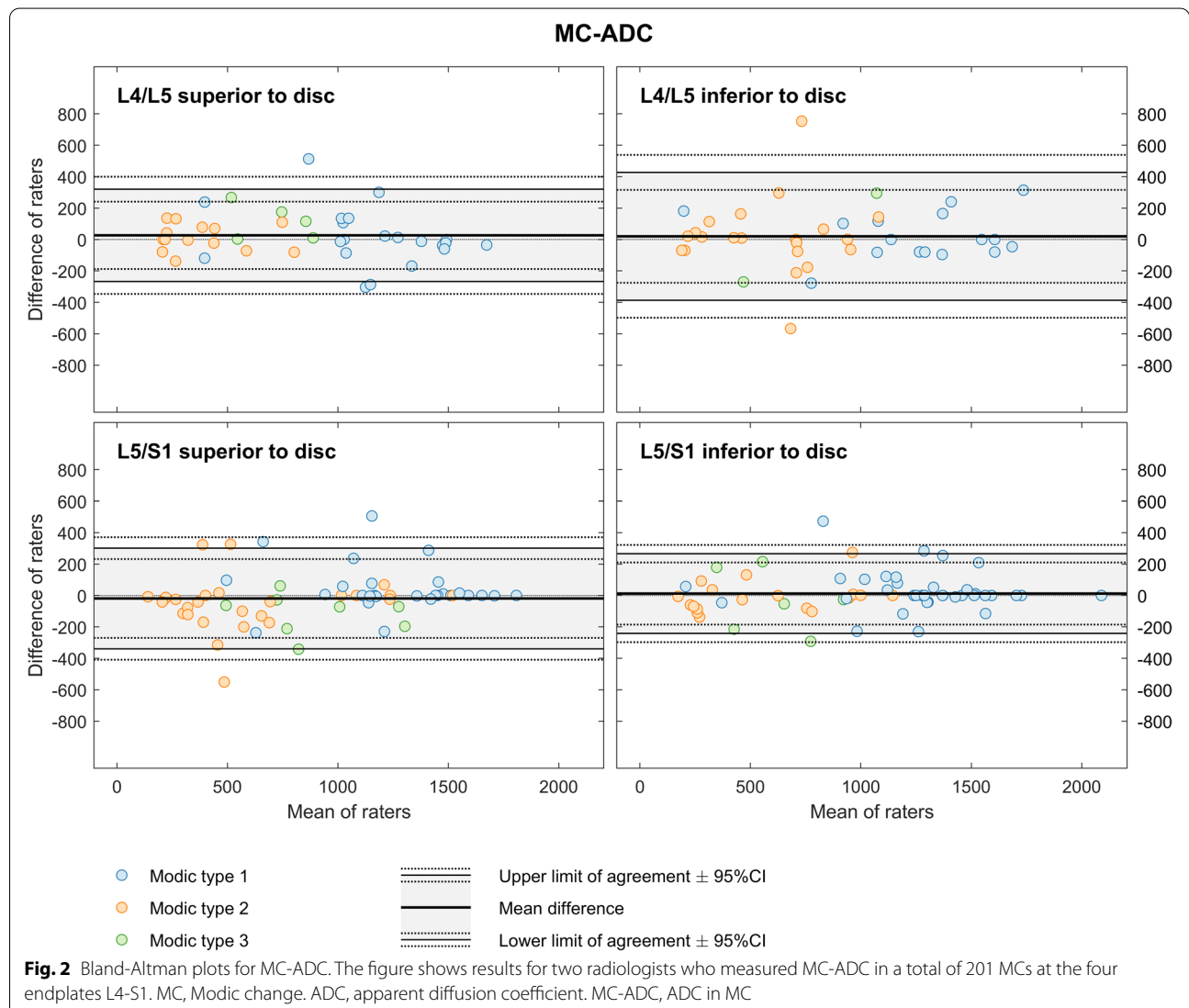
Tabled values are numbers (%)

Table 4 Interobserver reliability for ADC variables

| | L4/L5 superior to disc, n = 40 | L4/L5 inferior to disc, n = 39 | L5/S1 superior to disc, n = 62 | L5/S1 inferior to disc, n = 60 |
|--------------|--------------------------------|--------------------------------|--------------------------------|--------------------------------|
| MC-ADC | 0.97 (0.94–0.98) | 0.95 (0.90–0.97) | 0.97 (0.94–0.98) | 0.98 (0.97–0.99) |
| MC-ADC% | 0.94 (0.86–0.97) | 0.91 (0.84–0.96) | 0.96 (0.94–0.98) | 0.97 (0.95–0.98) |
| MC-ADC-ratio | 0.86 (0.74–0.92) | 0.87 (0.75–0.93) | 0.84 (0.75–0.91) | 0.84 (0.73–0.90) |

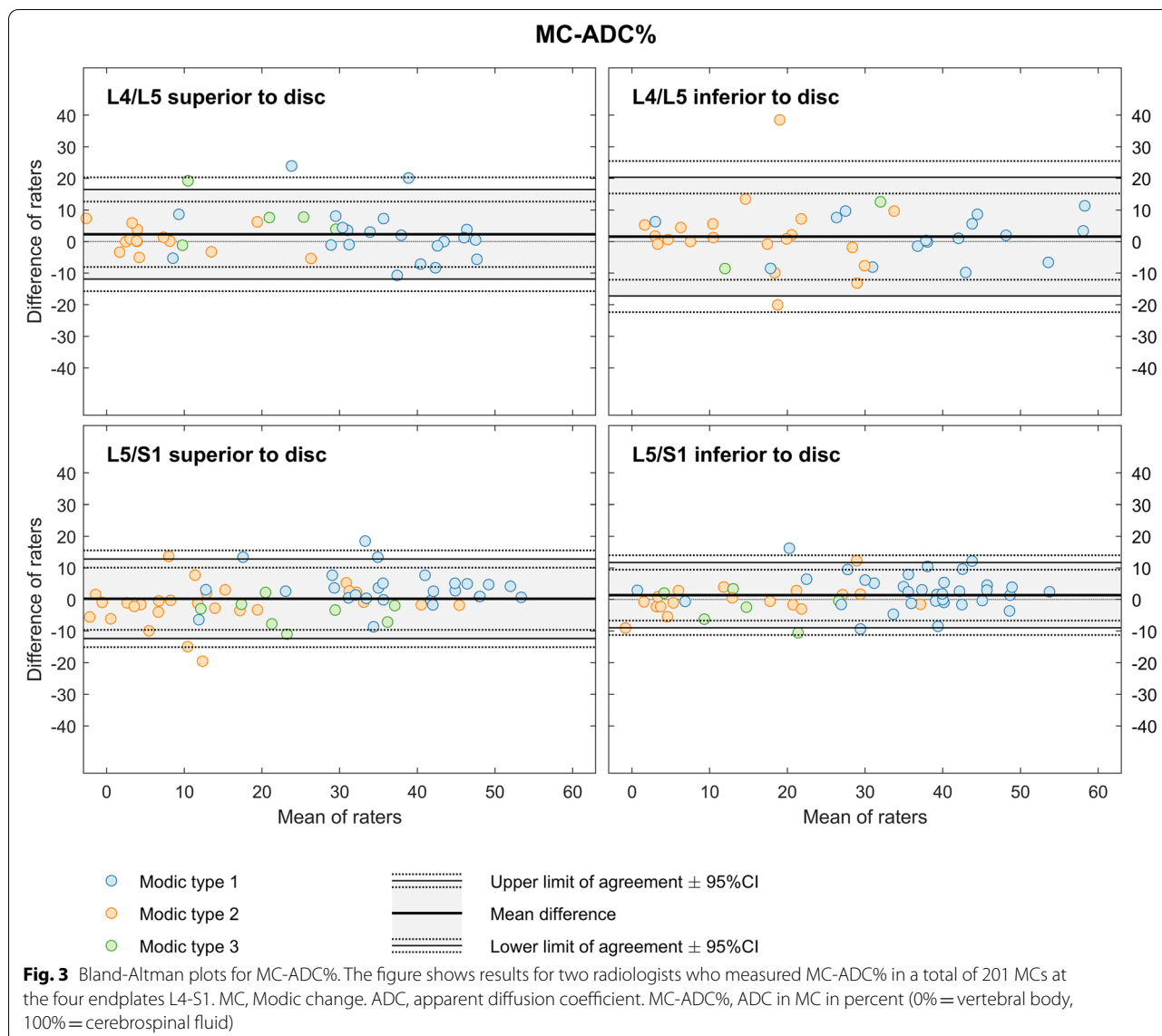
ADC Apparent diffusion coefficient, MC Modic change. MC-ADC, ADC in MC. MC-ADC%, ADC in MC in percent (0% = vertebral body, 100% = cerebrospinal fluid). MC-ADC-ratio, ADC in MC divided by ADC in normal vertebral body marrow

Values are intraclass correlation coefficients (95% confidence intervals)



The difference between the two observers was > 50% of their pairwise mean in 18 (9%) of the 201 MCs for MC-ADC, 41 MCs (20%) for MC-ADC%, and 34 MCs (17%) for MC-ADC-ratio.

Reproducibility parameters for ADC values in CSF and normal vertebral body marrow are shown in Additional file 1, Table A2.



ADC values by MC type group

Unadjusted mean values of the three MC related ADC variables are shown in Table 5.

Adjusted for data dependency within patients in the linear mixed-effects models, the predicted means for the ADC variables were higher in the type 1 vs type 3 MC group and in the type 3 vs type 2 MC group ($p \leq 0.001$ to 0.02) (Fig. 5).

Predicted mean for type 1 vs 3 vs 2 was for MC-ADC ($10^{-6} \text{ mm}^2/\text{s}$) 1201 vs 796 vs 576, for MC-ADC% 36 vs 21 vs 14, and for MC-ADC-ratio 5.9 vs 4.2 vs 3.1.

The ability to discriminate between the MC type groups was moderate to high for MC-ADC and MC-ADC% (AUC 0.73–0.91) and low to moderate for MC-ADC-ratio (AUC 0.67–0.85) (Fig. 6).

Supplementary ADC data are found in Additional file 1, Table A3 and Fig. A1.

Discussion

This study provides new data on interobserver reproducibility for ADC values in MCs. We found relatively better reproducibility for MC-ADC than for MC-ADC% and MC-ADC-ratio. To our knowledge, this is also the first study to show higher ADC values for a type 1 vs a type 3 MC group and for a type 3 vs a pure type 2 MC group, supporting our hypothesis based on histology of MCs [10, 16, 21].

We tested the hypothesis of ADC differences between MC types to assess the construct validity of the ADC variables [26, 27]. ADC maps cannot replace images

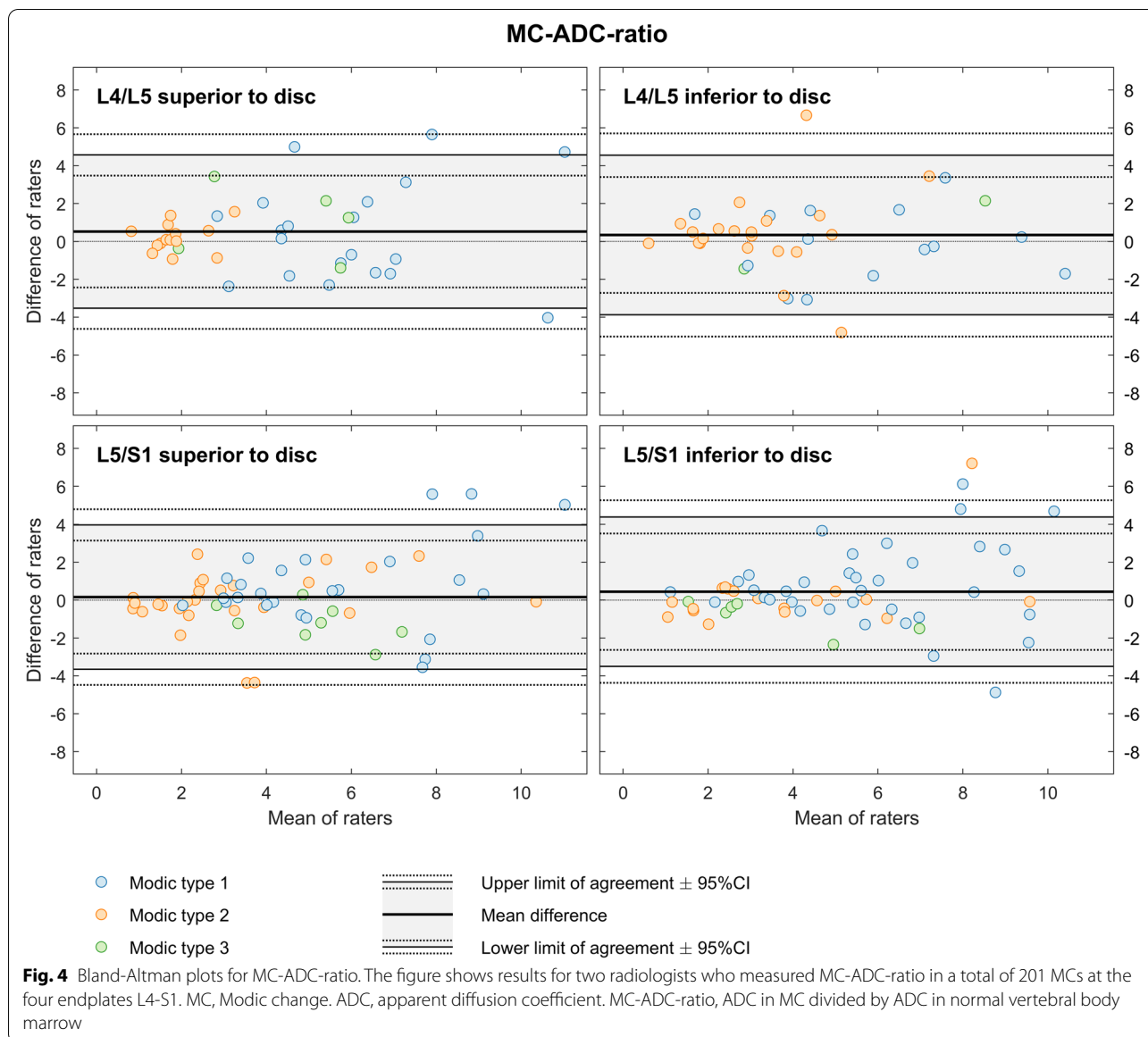


Table 5 Unadjusted mean for ADC variables by Modic type group

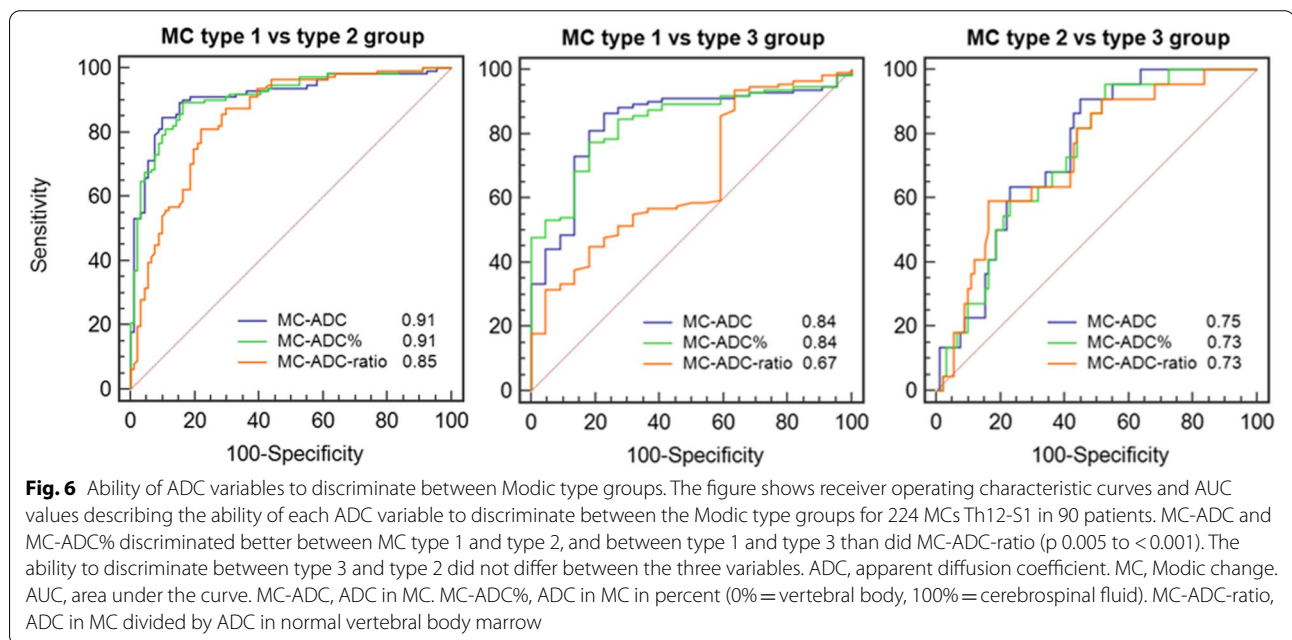
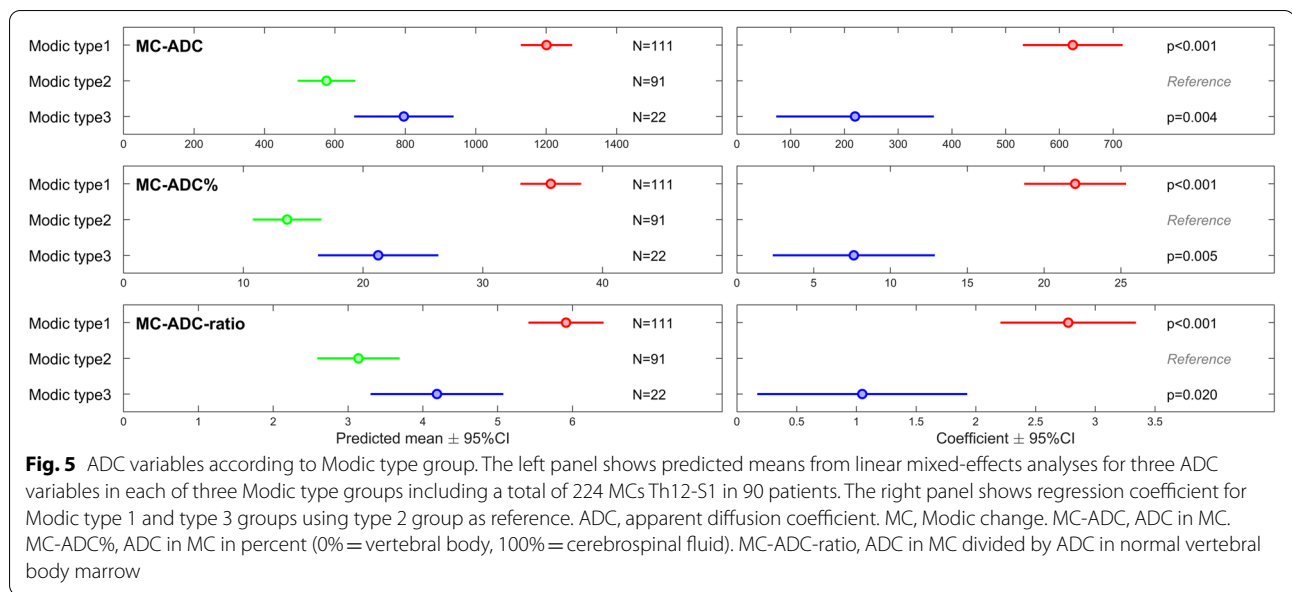
| Modic group | Number of MCs | MC-ADC | MC-ADC% | MC-ADC-ratio |
|-------------|---------------|------------|-------------|--------------|
| Type 1 | 111 | 1226 (352) | 36.3 (12.2) | 6.0 (2.5) |
| Type 2 | 91 | 535 (306) | 12.7 (11.1) | 3.0 (1.9) |
| Type 3 | 22 | 786 (290) | 21.1 (9.8) | 4.5 (1.9) |

ADC Apparent diffusion coefficient, MC Modic change. MC-ADC, ADC in MC. MC-ADC%, ADC in MC in percent (0% = vertebral body, 100% = cerebrospinal fluid). MC-ADC-ratio, ADC in MC divided by ADC in normal vertebral body marrow

Tabled are mean values (standard deviation) across Th12-S1 in each of three Modic type groups including a total of 224 MCs in 90 patients

used to discriminate between MC types. The discriminative ability still supports the validity of MC-ADC and MC-ADC% and weakens the validity of MC-ADC-ratio. To evaluate how well ADC values represent actual diffusion (criterion validity), one could perform DWI of phantoms with defined diffusion characteristics [28–30].

Pooled LoA suggested that 95% of differences in MC-ADC between observers can be expected to fall within $7 \pm 316 (10^{-6} \text{ mm}^2/\text{s})$. This is relevant when different observers measure MC-ADC in the same patient. $\text{ICC} \geq 0.95$ indicated that MC-ADC distinguished well between the patients [31], despite LoA reached 35% of the mean across L4-S1. The ICC quantifies the



between-subject variability in relation to the measurement error [31, 32]. Thus, the high ICC values (≥ 0.95) may reflect the large variability in MC-ADC values between the patients in our sample. In more homogeneous samples the ICC will be lower.

No previous study has reported specifically on the reproducibility of ADC values in MCs. A study of ADC measurements in active spondyloarthritis foci and type 1 MCs [6] reported interobserver ICCs of 0.89–0.98. Other studies on ADC values in bone marrow lacked

interobserver data [23, 33]. Our LoA for ADC in normal lumbar bone marrow ($4\% \pm 56\%$) (Additional file 1, Table A2) were only slightly wider than previously reported for intra observer LoA ($5\% \pm 45\%$) [23]. ADC values have been found to be less reproducible in bone marrow than in soft tissues [23]. Thus, our results seem to agree with relevant prior studies.

Standardized ROIs, pilot testing, and clear instructions for where to measure probably reduced the variability of the ADC measurements. MC-ADC implied

a single measurement, avoiding variation from measurements in CSF and normal bone marrow. This may partly explain the relatively better reproducibility for MC-ADC compared to MC-ADC% and MC-ADC-ratio. We included the two latter variables since it had been found useful in prior studies of ADC values to standardize lesion values against normal tissue values [34–36]. However, in our study this approach added variability. Compared to MC-ADC, MC-ADC-ratio also discriminated less well between the MC type groups. MC-ADC seems more feasible, reproducible, and promising for use in further research.

In line with our results, Belykh et al. found higher mean ADC ($10^{-6} \text{ mm}^2/\text{s}$) in type 1 vs type 2 MCs (498 vs 223, $p < 0.001$) [15]. Prior statistical comparisons of ADC values between all three MC type groups are lacking. In a study with 20 MCs, mean ADC (recalculated to $10^{-6} \text{ mm}^2/\text{s}$) was descriptively reported to be 624, 500, and 756 in type 1, 2, and 3 MCs, respectively [4]. Thus, ADC values differed between studies. Our mean ADC value of 1226 in type 1 MCs was midway in the range of previous values (498 to 1800) [4, 5, 15], and close to what was found in spondyloarthritis foci (1240) [36].

Many factors can affect ADC values in MCs, such as MRI technique (sequence parameters, b values, fat suppression) [37–40], ROI size and location, type of ADC measure (mean, percentile, histogram), and the definition of MC type (e.g., pure, mixed). Lack of information on mixed MC types, ROI size, and exact location of the ROI in the MC further complicates a comparison of the ADC values [5, 15].

Strengths and limitations

Strengths of this study are standardized MRI methodology, well-defined criteria for measuring ADC, and a large enough sample size to compare ADC values between MC type groups. A limitation is that our type 3 MC group was dominated by type 2/3 MCs, which may have reduced its ADC values. Partial volume effect can bias ADC measurements in MCs. This was likely a minor issue in our study, since 85% of the MCs appeared clearly larger (based on height ≥ 7 mm) than the slice thickness applied (4 mm) and at least as large as the ROI used (diameter 7 mm). The interobserver reliability for MC type group varied, reflecting difficulties in assessing signal intensities in MCs, especially in mixed MC types, which were prevalent (Table 3). The observers were experienced and had performed a pilot study. Interobserver differences may be larger between less experienced radiologists. We did not assess intra observer agreement, which is often better than the interobserver agreement [41–44].

The ADC maps showed some noise and distortion (Fig. 1), which are common problems in spine DWI [40].

The single-shot echo-planar imaging method applied is prone to susceptibility artefacts, which can influence ADC values. The DWI sequence (3 min 48 s) was part of an extensive MRI protocol where each sequence had been shortened to reduce total scan time and make the protocol feasible at all study centres. Longer acquisition time could have been used to improve the ADC maps [45, 46]. New DWI methods like RESOLVE (readout segmentation of long variable echo-trains), can also provide better image quality but were not available to us at the time [47]. The DWI method we used should be possible to apply at most MRI centres. Importantly, we used T1/T2 images as anatomical references when measuring ADC, and the modest quality of the ADC maps hardly affected the overall results.

Implications

Our findings have some implications for future research. Firstly, MC-ADC may be preferable when all study participants undergo identical DWI protocols. Secondly, the intra observer repeatability of the ADC variables and their reproducibility with other and improved DWI protocols should be clarified. Finally, the clinical relevance of measuring ADC in MCs is unknown and should be investigated, especially in the most inflammatory type 1 MC group. In inflammatory lesions of spondyloarthritis and sacroiliitis, ADC measures were related to disease activity [36, 48].

Conclusions

ADC values of MCs had overall moderate interobserver reproducibility and they differed between MC types as hypothesized. The reproducibility was best for MC-ADC - measured in a ROI of predefined size - without standardization against normal bone marrow or CSF. This variable appears feasible, reliable, and valid to use in further research.

Abbreviations

ADC: Apparent diffusion coefficient; AUC: Area under the curve; CSF: Cerebrospinal fluid; CI: Confidence interval; DWI: Diffusion weighted imaging; LoA: Limits of agreement; MCs: Modic Changes; MRI: Magnetic resonance imaging; ROI: Region of interest; SD: Standard deviation; T1/T2: T1- and T2-weighted non-fat saturated fast spin-echo images.

Supplementary Information

The online version contains supplementary material available at <https://doi.org/10.1186/s12891-022-05610-4>.

Additional file 1.

Additional file 2.

Additional file 3.

Acknowledgements

The authors thank their collaborators in the AIM-study group for their contributions.

Authors' contributions

MHD contributed to study design and acquisition and analysis of data, and drafted the manuscript. NV contributed to study design and acquisition and interpretation of data, and revised the manuscript critically. PMK contributed to acquisition and interpretation of data, and revised the manuscript critically. JAZ, KS, GB, JIB, LG and GHM contributed to interpretation of data and revised the manuscript critically. EA contributed to study design, MRI protocol, and interpretation of data and revised the manuscript critically. JA (statistical supervisor) contributed to analysis and interpretation of data. AE contributed to study design, acquisition and analysis of data, and drafting of the manuscript. All authors read and approved the final manuscript.

Funding

Open access funding provided by University of Bergen. This study was funded by KLINBEFORSK (grant no. 2017–201), the Western Norway Regional Health Authority (grant nos. HV 911891 and HV 911938), and the South East Norway Regional Health Authority (grant no. 2015–090). Source of funds had no role in study design; collection, analysis, and interpretation of data; writing of the report; or the decision to submit the report for publication.

Availability of data and materials

Requests to access data should be addressed to kjersti.storheim@medisin.uio.no. De-identified individual participant data will be available to medical researchers by request in accordance with local legislation and ethical approval. All proposals requesting data access will need to specify an analysis plan and will need approval of the scientific board before any data can be released.

Declarations

Ethics approval and consent to participate

The study was performed in accordance with the Declaration of Helsinki and was approved by the Regional Committees for Medical Research Ethics in South East Norway (ref. no. 2014/158). All patients gave written informed consent prior to inclusion.

Consent for publication

Not applicable.

Competing interests

The authors declare that they have no conflict of interests.

Author details

¹Department of Radiology, Haukeland University Hospital, Jonas Liesvei 65, 5021 Bergen, Norway. ²Department of Clinical Medicine, University of Bergen, P.O. Box 7804, 5020 Bergen, Norway. ³Research and Communication Unit for Musculoskeletal Health (FORMI), Division of Neuroscience, Oslo University Hospital HF, Ullevål, Bygg 37b, P.O. Box 4956, Nydalen, 0424 Oslo, Norway. ⁴Faculty of Medicine, University of Oslo, P.O. Box 1072 Blindern, 0316 Oslo, Norway. ⁵Faculty of Health Science, OsloMet - Oslo Metropolitan University, P.O. Box 4, St. Olavs plass, 0130 Oslo, Norway. ⁶Department of Rheumatology, University Hospital of North Norway, P.O. Box 100, 9038 Tromsø, Norway. ⁷Department of Physical Medicine and Rehabilitation, Oslo University Hospital HF, P.O. Box 4956 Nydalen, 0424 Oslo, Norway. ⁸Department of Rheumatology, Østfold Hospital Trust, P.O. Box 300, 1714 Grålum, Moss, Norway. ⁹Department of Physical Medicine and Rehabilitation, St. Olavs Hospital, Trondheim University Hospital, P.O. Box 3250 Torgarden, 7006 Trondheim, Norway. ¹⁰Department of Neuromedicine and Movement Science, Norwegian University of Science and Technology (NTNU), 7491 Trondheim, Norway. ¹¹Department of Clinical Engineering, Haukeland University Hospital, P.O. Box 1400, 5021 Bergen, Norway. ¹²Centre for Clinical Research, Haukeland University Hospital, Jonas Liesvei 65, 5021 Bergen, Norway.

Received: 24 February 2022 Accepted: 29 June 2022

Published online: 22 July 2022

References

1. Padhani AR, Liu G, Koh DM, Chenevert TL, Thoeny HC, Takahara T, et al. Diffusion-weighted magnetic resonance imaging as a cancer biomarker: consensus and recommendations. *Neoplasia*. 2009;11(2):102–25.
2. Dallaudiere B, Lecouvet F, Vande Berg B, Omoumi P, Perlepe V, Cerny M, et al. Diffusion-weighted MR imaging in musculoskeletal diseases: current concepts. *Diagn Interv Imaging*. 2015;96(4):327–40.
3. Khoo MM, Tyler PA, Saifuddin A, Padhani AR. Diffusion-weighted imaging (DWI) in musculoskeletal MRI: a critical review. *Skelet Radiol*. 2011;40(6):665–81.
4. Eguchi Y, Ohtori S, Yamashita M, Yamauchi K, Suzuki M, Orita S, et al. Diffusion magnetic resonance imaging to differentiate degenerative from infectious endplate abnormalities in the lumbar spine. *Spine (Phila Pa 1976)*. 2011;36(3):E198–202.
5. Daghighi MH, Poureisa M, Safarpour M, Behzadmehr R, Fouladi DF, Meshkini A, et al. Diffusion-weighted magnetic resonance imaging in differentiating acute infectious spondylitis from degenerative Modic type 1 change; the role of b-value, apparent diffusion coefficient, claw sign and amorphous increased signal. *Br J Radiol*. 2016;89(1066):20150152.
6. Dallaudiere B, Dautry R, Preux PM, Perozziello A, Lincot J, Schouman-Claeys E, et al. Comparison of apparent diffusion coefficient in spondylarthrosis axial active inflammatory lesions and type 1 Modic changes. *Eur J Radiol*. 2014;83(2):366–70.
7. Patel KB, Poplawski MM, Pawha PS, Naidich TP, Tanenbaum LN. Diffusion-weighted MRI "claw sign" improves differentiation of infectious from degenerative modic type 1 signal changes of the spine. *AJNR Am J Neuroradiol*. 2014;35(8):1647–52.
8. Suh CH, Yun SJ, Jin W, Lee SH, Park SY, Ryu CW. ADC as a useful diagnostic tool for differentiating benign and malignant vertebral bone marrow lesions and compression fractures: a systematic review and meta-analysis. *Eur Radiol*. 2018;28(7):2890–902.
9. Sartoretti E, Sartoretti-Schefer S, van Smoorenburg L, Eichenberger B, Schwenk A, Czell D, et al. Single shot zonal oblique multislice SE-EPI diffusion-weighted imaging with low to ultra-high b-values for the differentiation of benign and malignant vertebral spinal fractures. *Eur J Radiol Open*. 2021;8:100377.
10. Modic MT, Steinberg PM, Ross JS, Masaryk TJ, Carter JR. Degenerative disk disease: assessment of changes in vertebral body marrow with MR imaging. *Radiology*. 1988;166(1 Pt 1):193–9.
11. Splendiani A, Bruno F, Marsecano C, Arrigoni F, Di Cesare E, Barile A, et al. Modic I changes size increase from supine to standing MRI correlates with increase in pain intensity in standing position: uncovering the "biomechanical stress" and "active discopathy" theories in low back pain. *Eur Spine J*. 2019;28(5):983–92.
12. Maatta JH, Karppinen J, Paananen M, Bow C, Luk KD, Cheung KM, et al. Refined phenotyping of Modic changes: imaging biomarkers of prolonged severe low back pain and disability. *Medicine (Baltimore)*. 2016;95(22):e3495.
13. Saukkonen J, Maatta J, Oura P, Kyllonen E, Tervonen O, Niinimäki J, et al. Association between Modic changes and low back pain in middle age: a northern Finland birth cohort study. *Spine (Phila Pa 1976)*. 2020;45(19):1360–7.
14. Herlin C, Kjaer P, Espeland A, Skouen JS, Leboeuf-Yde C, Karppinen J, et al. Modic changes—their associations with low back pain and activity limitation: a systematic literature review and meta-analysis. *PLoS One*. 2018;13(8):e0200677.
15. Belykh E, Kalinin AA, Patel AA, Miller EJ, Bohl MA, Stepanov IA, et al. Apparent diffusion coefficient maps in the assessment of surgical patients with lumbar spine degeneration. *PLoS One*. 2017;12(8):e0183697.
16. Dudli S, Fields AJ, Samartzis D, Karppinen J, Lotz JC. Pathobiology of Modic changes. *Eur Spine J*. 2016;25(11):3723–34.
17. Braten LCH, Rolfsen MP, Espeland A, Wigemyr M, Assmus J, Froholdt A, et al. Efficacy of antibiotic treatment in patients with chronic low back pain and Modic changes (the AIM study): double blind, randomised, placebo controlled, multicentre trial. *BMJ*. 2019;367:l5654.
18. Storheim K, Espeland A, Grovle L, Skouen JS, Assmus J, Anke A, et al. Antibiotic treatment in patients with chronic low back pain and Modic changes (the AIM study): study protocol for a randomised controlled trial. *Trials*. 2017;18(1):596.

19. Kottner J, Audige L, Brorson S, Donner A, Gajewski BJ, Hrobjartsson A, et al. Guidelines for reporting reliability and agreement studies (GRRAS) were proposed. *J Clin Epidemiol*. 2011;64(1):96–106.
20. Kristoffersen PM, Vetti N, Storheim K, Braten LC, Rolfsen MP, Assmus J, et al. Short tau inversion recovery MRI of Modic changes: a reliability study. *Acta Radiol Open*. 2020;9(1):2058460120902402.
21. Perilli E, Parkinson IH, Truong LH, Chong KC, Fazzalari NL, Osti OL. Modic (endplate) changes in the lumbar spine: bone micro-architecture and remodelling. *Eur Spine J*. 2015;24(9):1926–34.
22. Sim J, Wright CC. The kappa statistic in reliability studies: use, interpretation, and sample size requirements. *Phys Ther*. 2005;85(3):257–68.
23. Michoux NF, Ceranka JW, Vandemeulebroucke J, Peeters F, Lu P, Absil J, et al. Repeatability and reproducibility of ADC measurements: a prospective multicenter whole-body-MRI study. *Eur Radiol*. 2021;31(7):4514–27.
24. Koo TK, Li MY. A guideline of selecting and reporting Intraclass correlation coefficients for reliability research. *J Chiropr Med*. 2016;15(2):155–63.
25. Kang SK, Zhang A, Pandharipande PV, Chandarana H, Braithwaite RS, Littenberg B. DWI for renal mass characterization: systematic review and Meta-analysis of diagnostic test performance. *AJR Am J Roentgenol*. 2015;205(2):317–24.
26. Malattia C, Damasio MB, Pistorio A, Ioseliani M, Vilca I, Valle M, et al. Development and preliminary validation of a paediatric-targeted MRI scoring system for the assessment of disease activity and damage in juvenile idiopathic arthritis. *Ann Rheum Dis*. 2011;70(3):440–6.
27. Terwee CB, Bot SD, de Boer MR, van der Windt DA, Knol DL, Dekker J, et al. Quality criteria were proposed for measurement properties of health status questionnaires. *J Clin Epidemiol*. 2007;60(1):34–42.
28. McHugh DJ, Zhou FL, Wimpenny I, Poologasundarampillai G, Naish JH, Hubbard Cristinacce PL, et al. A biomimetic tumor tissue phantom for validating diffusion-weighted MRI measurements. *Magn Reson Med*. 2018;80(1):147–58.
29. Nilsson M, Larsson J, Lundberg D, Szczepankiewicz F, Witzel T, Westin CF, et al. Liquid crystal phantom for validation of microscopic diffusion anisotropy measurements on clinical MRI systems. *Magn Reson Med*. 2018;79(3):1817–28.
30. Fieremans E, Lee HH. Physical and numerical phantoms for the validation of brain microstructural MRI: a cookbook. *Neuroimage*. 2018;182:39–61.
31. de Vet HCW, Terwee CB, Knol DL, Bouter LM. When to use agreement versus reliability measures. *J Clin Epidemiol*. 2006;59(10):1033–9.
32. Bartlett JW, Frost C. Reliability, repeatability and reproducibility: analysis of measurement errors in continuous variables. *Ultrasound Obstet Gynecol*. 2008;31(4):466–75.
33. Moller JM, Ostergaard M, Thomsen HS, Sorensen IJ, Madsen OR, Pedersen SJ. Test-retest repeatability of the apparent diffusion coefficient in sacroiliac joint MRI in patients with axial spondyloarthritis and healthy individuals. *Acta Radiol Open*. 2020;9(3):2058460120906015.
34. Soyer P, Kanematsu M, Taouli B, Koh DM, Manfredi R, Vilgrain V, et al. ADC normalization: a promising research track for diffusion-weighted MR imaging of the abdomen. *Diagn Interv Imaging*. 2013;94(6):571–3.
35. Uto T, Takehara Y, Nakamura Y, Naito T, Hashimoto D, Inui N, et al. Higher sensitivity and specificity for diffusion-weighted imaging of malignant lung lesions without apparent diffusion coefficient quantification. *Radiology*. 2009;252(1):247–54.
36. Lee KH, Chung HY, Xu X, Lau VWH, Lau CS. Apparent diffusion coefficient as an imaging biomarker for spinal disease activity in axial Spondyloarthritis. *Radiology*. 2019;291(1):121–8.
37. Chenevert TL, Galban CJ, Ivancevic MK, Rohrer SE, Londy FJ, Kwee TC, et al. Diffusion coefficient measurement using a temperature-controlled fluid for quality control in multicenter studies. *J Magn Reson Imaging*. 2011;34(4):983–7.
38. Fedeli L, Belli G, Ciccarone A, Coniglio A, Esposito M, Giannelli M, et al. Dependence of apparent diffusion coefficient measurement on diffusion gradient direction and spatial position - a quality assurance intercomparison study of forty-four scanners for quantitative diffusion-weighted imaging. *Phys Med*. 2018;55:135–41.
39. Belli G, Busoni S, Ciccarone A, Coniglio A, Esposito M, Giannelli M, et al. Quality assurance multicenter comparison of different MR scanners for quantitative diffusion-weighted imaging. *J Magn Reson Imaging*. 2016;43(1):213–9.
40. Oner AY, Tali T, Celikyay F, Celik A, Le Roux P. Diffusion-weighted imaging of the spine with a non-carr-Purcell-meiboom-gill single-shot fast spin-echo sequence: initial experience. *AJNR Am J Neuroradiol*. 2007;28(3):575–80.
41. Moreau B, Iannesi A, Hoog C, Beaumont H. How reliable are ADC measurements? A phantom and clinical study of cervical lymph nodes. *Eur Radiol*. 2018;28(8):3362–71.
42. Pei Y, Xie S, Li W, Peng X, Qin Q, Ye Q, et al. Evaluation of simultaneous-multislice diffusion-weighted imaging of liver at 3.0 T with different breathing schemes. *Abdom Radiol (NY)*. 2020;45(11):3716–29.
43. Lu TL, Meuli RA, Marques-Vidal PM, Bize P, Denys A, Schmidt S. Interobserver and intraobserver variability of the apparent diffusion coefficient in treated malignant hepatic lesions on a 3.0T machine: measurements in the whole lesion versus in the area with the most restricted diffusion. *J Magn Reson Imaging*. 2010;32(3):647–53.
44. Petralia G, Bonello L, Summers P, Preda L, Malasevski A, Raimondi S, et al. Intraobserver and interobserver variability in the calculation of apparent diffusion coefficient (ADC) from diffusion-weighted magnetic resonance imaging (DW-MRI) of breast tumours. *Radiol Med*. 2011;116(3):466–76.
45. Winfield JM, Payne GS, Weller A, deSouza NM. DCE-MRI, DW-MRI, and MRS in Cancer: challenges and advantages of implementing qualitative and quantitative multi-parametric imaging in the clinic. *Top Magn Reson Imaging*. 2016;25(5):245–54.
46. Koh DM, Blackledge M, Padhani AR, Takahara T, Kwee TC, Leach MO, et al. Whole-body diffusion-weighted MRI: tips, tricks, and pitfalls. *AJR Am J Roentgenol*. 2012;199(2):252–62.
47. Xie M, Ren Z, Bian D, Li D, Yu L, Zhu F, et al. High resolution diffusion-weighted imaging with readout segmentation of long variable echo-trains for determining myometrial invasion in endometrial carcinoma. *Cancer Imaging*. 2020;20(1):66.
48. Zhang H, Huang H, Zhang Y, Tu Z, Xiao Z, Chen J, et al. Diffusion-weighted MRI to assess Sacroiliitis: improved image quality and diagnostic performance of readout-segmented Echo-planar imaging (EPI) over conventional single-shot EPI. *AJR Am J Roentgenol*. 2021;217(2):450–9.

Publisher's Note

Springer Nature remains neutral with regard to jurisdictional claims in published maps and institutional affiliations.

Ready to submit your research? Choose BMC and benefit from:

- fast, convenient online submission
- thorough peer review by experienced researchers in your field
- rapid publication on acceptance
- support for research data, including large and complex data types
- gold Open Access which fosters wider collaboration and increased citations
- maximum visibility for your research: over 100M website views per year

At BMC, research is always in progress.

Learn more biomedcentral.com/submissions

